

**Standardized Expression of  $^{18}\text{F}$ -NAV4694 and  $^{11}\text{C}$ -PiB  $\beta$ -Amyloid PET Results  
with the Centiloid Scale.**

Christopher C. Rowe,<sup>1,2</sup> Gareth Jones,<sup>1</sup> Vincent Doré,<sup>1,3</sup> Svetlana Pejoska,<sup>1</sup> Laura  
Margison,<sup>1</sup> Rachel S. Mulligan,<sup>1</sup> J. Gordon Chan,<sup>1</sup> Kenneth Young,<sup>1</sup> Victor L.  
Villemagne.<sup>1,2,4</sup>

*1. Department of Molecular Imaging, Austin Health, Melbourne, Australia.*

*2. Department of Medicine, The University of Melbourne, Melbourne, Australia.*

*3. CSIRO Health and Biosecurity, Brisbane, Australia*

*4. Florey Institute of Neuroscience and Mental Health, University of Melbourne,  
Melbourne, Australia.*

Corresponding and First Author:

Prof. Christopher Rowe MD FRACP

Department of Molecular Imaging

Austin Health

Studley Road

Heidelberg, Melbourne,

Victoria 3084,

Australia.

Email: [Christopher.rowe@austin.org.au](mailto:Christopher.rowe@austin.org.au)

Phone: 61 3 94965183

Fax: 61 3 94965663

**Disclaimer:**

Rowe has received research grants for imaging in dementia from Bayer-Schering Pharma, Avid Radiopharmaceuticals, GE Healthcare, Piramal, Astra Zeneca and Navidea. He has been a consultant or paid speaker at sponsored conference sessions for Bayer Schering Pharma, Piramal, GE Healthcare, Astra Zeneca, Roche and Janssen. Villemagne has been a consultant or paid speaker at sponsored conference sessions for Bayer Schering Pharma, Piramal, GE Healthcare, Astra Zeneca and Novartis. Co-authors Jones, Doré, Pejoska, Margison, Mulligan, Chan and Young have nothing to declare.

The study was partially supported by Project Grants 1044361 and 1071430 from the National Health Medical Research Council (NHMRC) of Australia, and by a research grant for imaging in dementia from Navidea.

The funding sources had no input into the design and conduct of the study; collection, management, analysis and interpretation of the data; and in the preparation, review, approval or decision to submit the manuscript for publication.

**Word Count: 3,813**

**Short Running Title:** Converting NAV4694 to Centiloid Units

## ABSTRACT

A common quantitative output value for  $\beta$ -amyloid ( $A\beta$ ) imaging across tracers and methods will allow better comparison of data across sites and application of universal diagnostic and prognostic values. A method has recently been developed that generates a unit of measurement called the Centiloid (*Klunk et al, Alzheimers Dement, 2015*). We applied this method on  $^{18}\text{F}$ -NAV4694 (NAV4694) and  $^{11}\text{C}$ -PiB (PiB)  $A\beta$  images to derive the scaling factor required to express tracer binding in Centiloids (CL).

**Methods:** Fifty-five participants, including 10 healthy young controls ( $33\pm 7$  yo), underwent both PiB and NAV4694 imaging with less than 3 months between scans. Images were acquired from 50 to 70 min post injection. Spatially normalized images were analyzed using the standard Centiloid method and regions (cortex and whole cerebellum reference) downloaded from the Global Alzheimer's Association Interactive Network website (<http://www.gaain.org>).

**Results:** Tracer binding was highly correlated ( $\text{SUVR}_{\text{NAV4694}} = 1.09 \times \text{SUVR}_{\text{PiB}} - 0.08$ ,  $R^2 = 0.99$ ). The equation to convert NAV4694 ( $\text{CL} = 100 \times (\text{SUVR}_{\text{NAV4694}} - 1.028)/1.174$ ) was similar to the published equation for PiB ( $\text{CL} = 100 \times (\text{SUVR}_{\text{PiB}} - 1.009)/1.067$ ). NAV4694 variance in the young controls compared to PiB was 0.85 ( $\text{SD}_{\text{NAV4694}}/\text{SD}_{\text{PiB}}$ ).

**Conclusions:** Both PiB and NAV4694 results can now be expressed in Centiloids, an important step that should allow better clinical and research use of  $A\beta$  imaging. The standard Centiloid method also showed that NAV4694 has slightly higher  $A\beta$

binding and lower variance than PiB, important properties for detecting early A $\beta$  deposition and change over time.

## **Introduction**

There is wide variability in the numbers and methods used to report quantitative measures of beta-amyloid ( $A\beta$ ) tracer binding in the brain measured with positron emission tomography (PET) (1). Results vary for each of the available tracers due to differences in both their specific and non-specific binding properties and recommended reference regions (2-5). Results are also influenced by the timing of scan acquisition after administration of the  $A\beta$  tracer, duration of the acquisition, image reconstruction algorithms, partial volume correction if applied, choice and extent of cortical regions, and the quantitative method employed such as Standardized Uptake Value Ratio, Distribution Volume Ratio, Binding Potential, etc. (6-16). Consequently most imaging labs have had to derive a normal range for their method and tracers or rely on subjective visual reading .

This lack of consistency in image analysis methods and highly variable expression of the results impedes the pooling of data across sites and comparison of studies (17). Lack of standardization prevents the application of universal cut points for diagnostic and prognostic purposes (18). It also limits comparison of the relative effectiveness of therapies that claim to reduce  $A\beta$  burden (17).

An international working party of  $A\beta$  imaging researchers has developed a method to standardize quantitative  $A\beta$  imaging measures by scaling the outcome to the Centiloid (CL) scale (18). This scale has a zero CL point that corresponds to the mean result obtained from scans in young adults who, based on age, are reasonably

assumed to be free of A $\beta$  plaques. The 100 CL point corresponds to the mean result of scans performed in a group of patients with typical Alzheimer's disease (AD) of mild severity, the time when A $\beta$  burden peaks in the course of AD (19, 20). Consequently, the measurement units for this scale have been named to reflect the 100-point scale and the application to amyloid, hence the term "Centiloid".

The data required to convert <sup>11</sup>C-PiB (PiB) A $\beta$  PET to Centiloid units (CL) is available from the Global Alzheimer's Association Interactive Network (GAAIN) website (<http://www.gaain.org>). The website provides free access to a standard cortical volume of interest (VOI) that covers the areas of significant <sup>11</sup>C-PiB A $\beta$  tracer binding in AD (Figure 1a) and a whole cerebellum VOI (Figure 1b) to use as the reference region. The standard cortical template was derived from subtraction of the mean PiB image normalized in MNI-152 space with SPM8 from older healthy subjects from the mean image of a group of patients with Alzheimer's disease. The resultant subtraction VOI was smoothed and then thresholded to only include voxels with a difference of >1.05 SUVR units. This data-driven VOI includes frontal, temporal, parietal (including precuneus), cingulate, insular and anterior striatum grey matter. (Figure 1a) The linear equation required to convert the PiB SUVR obtained by the standard Centiloid method on any PiB scan acquired from 50-70 minutes post injection is supplied. Importantly a validation set of PiB scans and MRI is also supplied so that the user can confirm correct application of the method by comparison to the results supplied with the validation scans before analysing their own scans. It is then possible to derive an additional linear equation to convert the

results obtained from any preferred in-house analysis method to CL units by analysis of PiB images that have been converted to parametric CL images by the standard Centiloid method (18).

To perform the conversion from SUVR to CL for tracers other than PiB (e.g.  $^{18}\text{F}$ -NAV4694), one site must first obtain matching PiB and  $^{18}\text{F}$ -NAV4694 (NAV4694) PET scans from the same individuals according to the standard Centiloid method as described by Klunk and colleagues (18). This data is then made available through GAAIN so that other sites can convert their own NAV4694 PET results to CL units without the need to perform matching PiB scans. The matched PiB and NAV4694 scans must cover the spectrum of A $\beta$  tracer binding from young healthy controls across the range of A $\beta$  burden up to and including patients with mild AD. By applying the standard Centiloid methods to these scans, a linear conversion equation (scaling factor) is derived that can then be used to express NAV4694 results in CL units. Other sites can then use the standard Centiloid method and regions of interest from the GAAIN site on their scans, and apply the scaling factor described in this manuscript to their NAV4694 scans to express their results in CL units. Furthermore, the site can then display a range of their scans as parametric images in CL units, apply their local analysis method and derive a second scaling factor that permits their usual in-house analysis method to transform their results into CL units (18).

<sup>18</sup>F-NAV4694 (formerly known as AZ4694) is an A $\beta$  imaging radiopharmaceutical that has nearly identical imaging characteristics to <sup>11</sup>C-PiB but with the convenience of fluorine-18 labelling (21, 22). The steric structure is very similar to PiB (Figure 2), and the time activity curves and blood clearance rates are similar (23). A head-to-head study in a range of normal older individuals and patients with mild cognitive impairment and AD, demonstrated near identical image appearance and neocortical SUVR to PiB (24). Like PiB, NAV4694 has higher specific cortical binding and lower non-specific white matter binding than has been reported with other F-18 labelled A $\beta$  radiopharmaceuticals (3, 23, 25, 26).

In this manuscript we describe the acquisition of the data and the derived scaling factor required to convert NAV4694 Standardized Uptake Value Ratios to Centiloid units.

## Materials and Methods

The study has been approved by the institutional review board of Austin Health, and all subjects signed an informed consent form.

### Subjects:

Paired  $^{11}\text{C}$ -PiB and  $^{18}\text{F}$ -NAV4694 PET scans were obtained in 55 subjects. The cohort comprised 10 healthy young controls acquired specifically for this study, and a previously published cohort of 25 healthy elderly controls, 10 patients with mild cognitive impairment, 7 patients with mild Alzheimer's disease and 3 patients with frontotemporal dementia (24). All subjects from the previously published cohort were included in this analysis. Demographics of the cohort are shown in Table 1.

### Scanning:

The paired PiB and NAV4694 PET scans for each individual were obtained within 3 months of each other and with a minimum of 2 hours between scans if  $^{11}\text{C}$ -PiB PET was done first or 24 hours if  $^{18}\text{F}$ -NAV4694 PET was done first. All scans were acquired on a Philips Allegro PET camera in 3D mode and processed with rotating Cs-137 point source attenuation correction. Image reconstruction used a 3D-RAMLA (row-action maximum likelihood algorithm) algorithm.

Participants were injected with 370 MBq of  $^{11}\text{C}$ -PiB and 250 MBq of  $^{18}\text{F}$ -NAV4694. As per the Centiloid standard protocol, the PiB acquisition was from 50-70 minutes post injection. This is also the optimal and recommended time for deriving SUVR with NAV4694 PET (23, 24) so the same imaging window was used for both tracers.

Examples of matched images with both tracers in a young healthy subject and a patient with mild AD are shown in Figure 3.

All subjects had MRI performed on a Siemens 3T Trio camera. The T1 MP-RAGE sequence with 1x1x1.2 mm voxels was used for image registration. Partial volume correction was not performed.

#### Image Analysis:

Each subject's MRI image was co-registered to the MNI-152 template with SPM8 and then each subjects PET was co-registered via the derived MRI transformation parameters using the SPM8 unified segmentation method, as described in detail in the Centiloid methodology paper (18). The standard Centiloid cortical and whole cerebellum reference VOI were downloaded from the GAAIN website (Figure 1) and applied to each scan.

The local processing pipeline was firstly validated on the standard PiB image set provided from the GAAIN website. Then the paired PiB and NAV4694 images were analysed with the standard method and Centiloid templates from GAAIN to derive SUVR measures that were plotted against each other. This produced the linear equation required to convert the standard NAV4694 SUVR to the equivalent or "calculated" PiB SUVR. ( $^{PiB-Calc}SUVR$ ) i.e.  $NAV4694\ SUVR = m \times (^{PiB}SUVR) + b$ ; so that by rearrangement of the equation  $^{PiB-Calc}SUVR = (NAV4694\ SUVR - b) / m$ .

As per the published standard Centiloid method, the conversion to Centiloid units was then accomplished by first converting the NAV4694 SUVR values into “PiB calculated” SUVR values as explained above, and then converting this result to CL.

Finally the equation to directly convert NAV4694 SUVR to CL was derived by plotting NAV4694 SUVR against the CL derived via conversion to <sup>PiB-Calcd</sup>SUVR.

The mean and variance of PiB and NAV4694 CL were compared in the young normal adults and the variance ratio was expressed as NAV4694 CL standard deviation (SD) divided by the PiB CL SD.

## Results

The validation of local implementation of the standard Centiloid method on the PiB scans supplied from the Centiloid GAAIN website gave a linear fit of  $CL_{Austin} = 1.00 * CL_{GAAIN} - 0.07$ , with  $R^2 = 0.9999$ . The fit exceeded the minimum specified acceptance criteria (i.e.  $R^2 > 0.98$ , slope 0.98-1.02, intercept between -2 and +2) (18) confirming that local implementation of the standard Centiloid method was accurate.

The locally acquired paired PiB and NAV4694 images were then analysed with the standard Centiloid templates and method and demonstrated a close linear correlation expressed by:  $SUVR_{NAV4694} = 1.09 \times SUVR_{PiB} - 0.08$ ,  $R^2 = 0.99$  (Figure 4). The strong correlation satisfied the Centiloid method criteria of a correlation between tracers of  $R^2 > 0.70$  to be valid for the CL process.

Conversion of the  $SUVR_{NAV4694}$  to the equivalent  $SUVR_{PiB}$  was performed using the above equation and those results were then transformed to CL (Figure 5). From this data the linear equation required to directly convert NAV4694 binding to CL was  $CL_{NAV4694} = 100 \times (SUVR_{NAV4694} - 1.028) / 1.174$ .

The mean and variance of the NAV4694 CL in the young adult normal subjects was  $-3.8 \pm 3.7$  CL compared to that found with PiB of  $-3.4 \pm 4.34$  yielding a variance ratio of 0.85 ( $SD_{NAV} / SD_{PiB}$ ).

## Discussion

The study demonstrated that the A $\beta$  imaging tracer NAV4694 has binding properties that allow conversion of SUVR output to Centiloids by linear transformation. The equation  $CL_{NAV4694} = 100 \times (SUVR_{NAV4694} - 1.028)/1.174$  enables NAV4694 scans acquired from 50 to 70 minutes post injection of tracer and analysed by the standard Centiloid method to be converted to CL without the need to collect paired PiB scans. Other sites may now apply this linear equation to their NAV4694 scans to derive CL values when NAV4694 SUVR has been calculated by the standard Centiloid method. The Centiloid method uses widely available, public domain programs to facilitate this process and makes available a standard data set for method validation. The NAV4694 and matched PiB scans used in this analysis have been uploaded to the Centiloid site on GAAIN to serve as a validation data set for other users.

An additional value of the standard Centiloid method is that it provides a mechanism to compare A $\beta$  tracers against PiB in a standard manner. The tight correlation of NAV4694 and PiB binding ( $R^2 = 0.99$ ) and the slope of this plot ( $SUVR_{NAV4694} = 1.09 \times SUVR_{PiB} - 0.08$ ) reveals that NAV4694 binding to A $\beta$  is very similar to PiB, even slightly higher. The variation in NAV4694 binding was also lower than PiB in young individuals with no A $\beta$ . This may be due to the higher count rate yielding better images during the scanning window given the longer physical decay half-life of 109 minutes for the  $^{18}F$  radiolabel on NAV4694 compared to the 20 minute physical half-life of the  $^{11}C$  radiolabel on PiB. These findings suggest that the longer half -life F-18 labelled NAV4694 may have not only advantages for efficient

production and use, but also may be better able to detect early A $\beta$  accumulation and small changes over time.

This study has not addressed the issue of regional tracer binding. However it is expected that regional CL values can be derived by creating CL parametric images using the global CL transformation before applying regions of interest. The value obtained from the voxels in a region of interest would then be in Centiloid units.

Ideally a site will reprocess their NAV4694 images using the standard Centiloid method and apply the conversion equation provided in this report to quantify their studies in Centiloid units. However, it may be possible to directly convert a local method global SUVR to CL by undertaking analysis of the standard NAV4694 data set that we have placed on the GAAIN website where, provided there is good correlation with the standard CL for these images ( $R^2 > 0.7$ ) (18), CL parametric images generated by the standard Centiloid method and regions can be used to derive a further linear transformation for locally preferred analysis methods to permit expression in CL.

In this study population, the mean PiB CL in young normal subjects was – 3.4 CL, so slightly below the anticipated mean of zero. This may be due to random variation in the study population but could be due to variation in the imaging equipment or image reconstruction methods used at the local site. In either case, it should not affect calculation of the conversion equation for NAV4694 SUVR to CL as the

effect was common to both the PiB and NAV4694 images. However, it may be that differences between PET systems and reconstruction methods might have a slight effect on use of the conversion equation when applied to other sites. Further work is needed to identify if this could be an issue for the Centiloid method and whether equipment specific equations may be needed.

### **Conclusions**

In summary, implementation of the Centiloid method for quantification of A $\beta$  PET output is an important step that should support better clinical and research use of A $\beta$  imaging. It will allow the use of multiple A $\beta$  tracers in studies such as multicenter, anti-A $\beta$  therapeutic trials and provide better diagnostic and prognostic data to clinicians by application of cut-points that are applicable to all A $\beta$  scans. Both PiB and NAV4694 measures of A $\beta$  burden can now be expressed in Centiloid units and the conversion equations for other tracers are expected to become available in the near future.

## **Disclosure**

First author Rowe has received research grants for imaging in dementia from Bayer, Avid Radiopharmaceuticals, GE Healthcare, Piramal, Astra Zeneca and Navidea. He has been a consultant or paid speaker at sponsored conference sessions for Bayer, Piramal, GE Healthcare, Astra Zeneca, Roche and Janssen. Senior author Villemagne has been a consultant or paid speaker at sponsored conference sessions for Bayer Schering Pharma, Piramal, GE Healthcare, Astra Zeneca and Novartis. Co-authors Jones, Doré, Pejoska, Margison, Mulligan, Chan and Young have nothing to declare. The study was partially supported by Project Grants 1044361 and 1071430 from the National Health Medical Research Council (NHMRC) of Australia, and by a research grant for imaging in dementia from Navidea. The funding sources had no input into the design and conduct of the study; collection, management, analysis and interpretation of the data; and in the preparation, review, approval or decision to submit the manuscript for publication.

## **Acknowledgements**

We thank Prof. Michael Woodward, Dr. John Merory, Ms. Fiona Lamb and the Brain Research Institute for their assistance with this study.

## REFERENCES

1. Rowe CC, Villemagne VL. Brain amyloid imaging. *J Nucl Med.* Nov 2011;52(11):1733-1740.
2. Clark CM, Pontecorvo MJ, Beach TG, et al. Cerebral PET with florbetapir compared with neuropathology at autopsy for detection of neuritic amyloid-beta plaques: a prospective cohort study. *Lancet Neurol.* Aug 2012;11(8):669-678.
3. Rowe CC, Ackerman U, Browne W, et al. Imaging of amyloid beta in Alzheimer's disease with 18F-BAY94-9172, a novel PET tracer: proof of mechanism. *Lancet Neurol.* Feb 2008;7(2):129-135.
4. Rowe CC, Ng S, Ackermann U, et al. Imaging beta-amyloid burden in aging and dementia. *Neurology.* May 15 2007;68(20):1718-1725.
5. Thurfjell L, Lundqvist R, Buckley C, Smith A, Sherwin P. Automated quantification of [18F]flutemetamol data - Comparison with standard of truth based on histopathology. *J Nucl Med.* 2013; 54((Supplement 2)):302.
6. Becker GA, Ichise M, Barthel H, et al. PET quantification of 18F-florbetaben binding to beta-amyloid deposits in human brains. *J Nucl Med.* May 2013;54(5):723-731.
7. Landau SM, Breault C, Joshi AD, et al. Amyloid-beta imaging with Pittsburgh compound B and florbetapir: comparing radiotracers and quantification methods. *J Nucl Med.* Jan 2013;54(1):70-77.

8. Lopresti BJ, Klunk WE, Mathis CA, et al. Simplified quantification of Pittsburgh Compound B amyloid imaging PET studies: a comparative analysis. *J Nucl Med.* Dec 2005;46(12):1959-1972.
9. Price JC, Klunk WE, Lopresti BJ, et al. Kinetic modeling of amyloid binding in humans using PET imaging and Pittsburgh Compound-B. *J Cereb Blood Flow Metab.* Nov 2005;25(11):1528-1547.
10. Mourik JE, Lubberink M, Schuitemaker A, et al. Image-derived input functions for PET brain studies. *Eur J Nucl Med Mol Imaging.* Mar 2009;36(3):463-471.
11. Tolboom N, Yaqub M, Boellaard R, et al. Test-retest variability of quantitative [11C]PIB studies in Alzheimer's disease. *Eur J Nucl Med Mol Imaging.* Oct 2009;36(10):1629-1638.
12. Yaqub M, Boellaard R, van Berckel BN, et al. Evaluation of Tracer Kinetic Models for Analysis of [(18)F]FDDNP Studies. *Mol Imaging Biol.* 2014; 16:136-45..
13. Zwan MD, Ossenkoppele R, Tolboom N, et al. Comparison of Simplified Parametric Methods for Visual Interpretation of 11C-Pittsburgh Compound-B PET Images. *J Nucl Med.* Jun 4 2014;55(8):1305-1307.
14. Mintun MA, Larossa GN, Sheline YI, et al. [11C]PIB in a nondemented population: potential antecedent marker of Alzheimer disease. *Neurology.* Aug 8 2006;67(3):446-452.
15. Schmidt ME, Chiao P, Klein G, et al. The influence of biological and technical factors on quantitative analysis of amyloid PET: Points to consider

and recommendations for controlling variability in longitudinal data. *Alzheimers Dement.* 2015; 11:1050-68..

16. Villemagne VL, O'Keefe G, Mulligan RS, Rowe CC. Quantitative approaches to amyloid imaging. *Methods Mol Biol.* 2011;680:201-225.
17. Carrillo MC, Rowe CC, Szoek C, et al. Research and standardization in Alzheimer's trials: reaching international consensus. *Alzheimers Dement.* Mar 2013;9(2):160-168.
18. Klunk WE, Koeppe RA, Price JC, et al. The Centiloid Project: standardizing quantitative amyloid plaque estimation by PET. *Alzheimers Dement.* Jan 2015;11(1):1-15 e11-14.
19. Villemagne VL, Burnham S, Bourgeat P, et al. Amyloid beta deposition, neurodegeneration, and cognitive decline in sporadic Alzheimer's disease: a prospective cohort study. *Lancet Neurol.* Apr 2013;12(4):357-367.
20. Jack CR, Jr., Wiste HJ, Lesnick TG, et al. Brain beta-amyloid load approaches a plateau. *Neurology.* Mar 5 2013;80(10):890-896.
21. Jureus A, Swahn BM, Sandell J, et al. Characterization of AZD4694, a novel fluorinated Abeta plaque neuroimaging PET radioligand. *J Neurochem.* Aug 2010;114(3):784-794.
22. Sundgren-Andersson AK, Svensson SPS, Swahn BM, et al. AZD4694: Fluorinated Positron Emission Tomography (PET) radioligand for detection of beta-amyloid deposits. *Alzheimers Dement.* 2009;5(4, Supplement 1):P267-P268 [abstract].

23. Cselenyi Z, Jonhagen ME, Forsberg A, et al. Clinical Validation of 18F-AZD4694, an Amyloid-beta-Specific PET Radioligand. *J Nucl Med.* Mar 2012;53(3):415-424.
24. Rowe CC, Pejoska S, Mulligan RS, et al. Head-to-head comparison of 11C-PiB and 18F-AZD4694 (NAV4694) for beta-amyloid imaging in aging and dementia. *J Nucl Med.* Jun 2013;54(6):880-886.
25. Vandenberghe R, Van Laere K, Ivanoiu A, et al. 18F-flutemetamol amyloid imaging in Alzheimer disease and mild cognitive impairment: a phase 2 trial. *Ann Neurol.* Sep 2010;68(3):319-329.
26. Wong DF, Rosenberg PB, Zhou Y, et al. In vivo imaging of amyloid deposition in Alzheimer disease using the radioligand 18F-AV-45 (florbetapir [corrected] F 18). *J Nucl Med.* Jun 2010;51(6):913-920.

**Table 1.** Demographics

<b>Group</b>	<b>n</b>	<b>Age (years)</b>	<b>MMSE</b>
Young Healthy Controls	10	33±7*	>28
Elderly Healthy Controls	25	74±8	29±1
Mild Cognitive Impairment	10	75±9	27±3*
Alzheimer's Disease	7	73±11	24±2*
Fronto-Temporal Dementia	3	68±5*	27±1*

\* Significantly different from Elderly Healthy Controls (p<0.05)

## FIGURES and LEGENDS

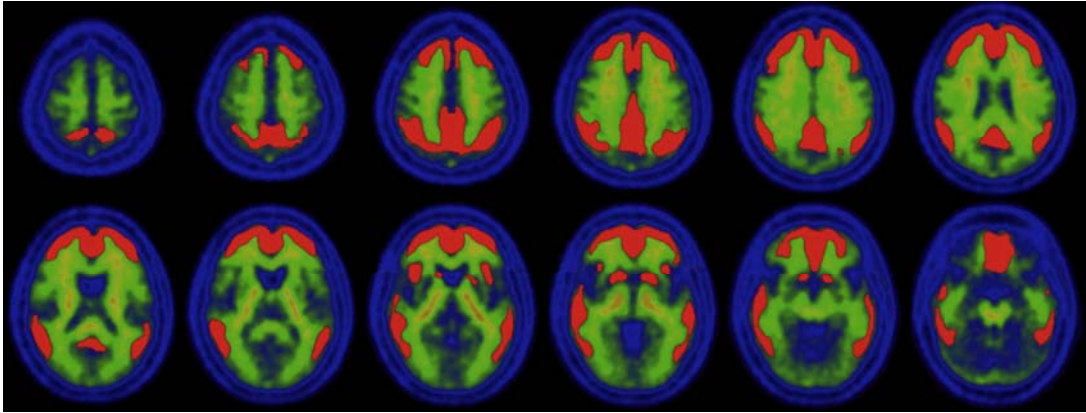


**Figure 1a.** The standard Centiloid method cortical volume of interest normalized to MNI-152 space. The whole cerebellum reference region is shown in figure 2b superimposed on the MNI-152 MRI template. Figure adapted from Klunk W, et al. Alzheimer's and Dementia, 2014.

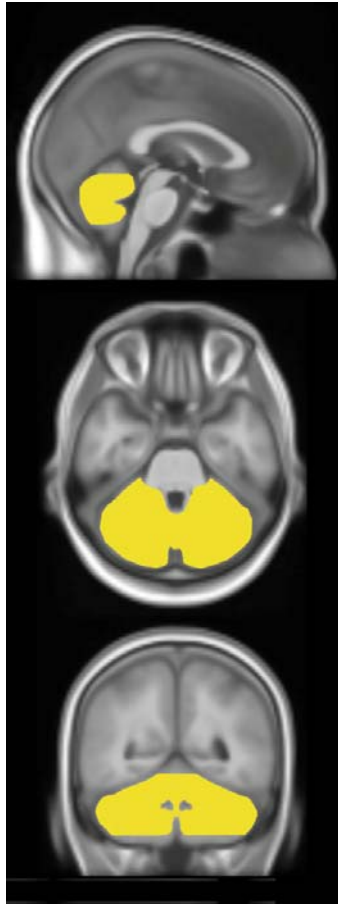


**Figure 1b.** Standard Centiloid method whole cerebellum reference region.

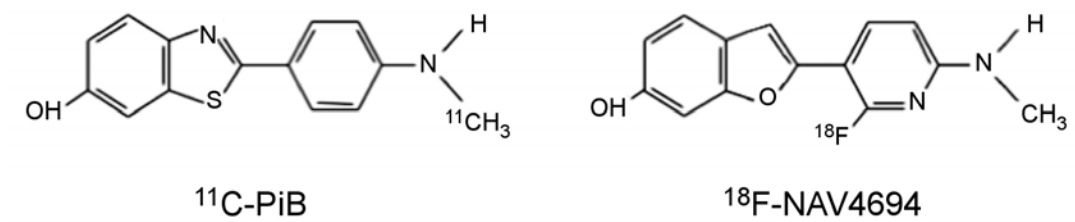


**Figure 2.** Chemical structures of  $^{11}\text{C}$ -PiB and  $^{18}\text{F}$ -NAV4694 (formerly  $^{18}\text{F}$ -AZD4694).

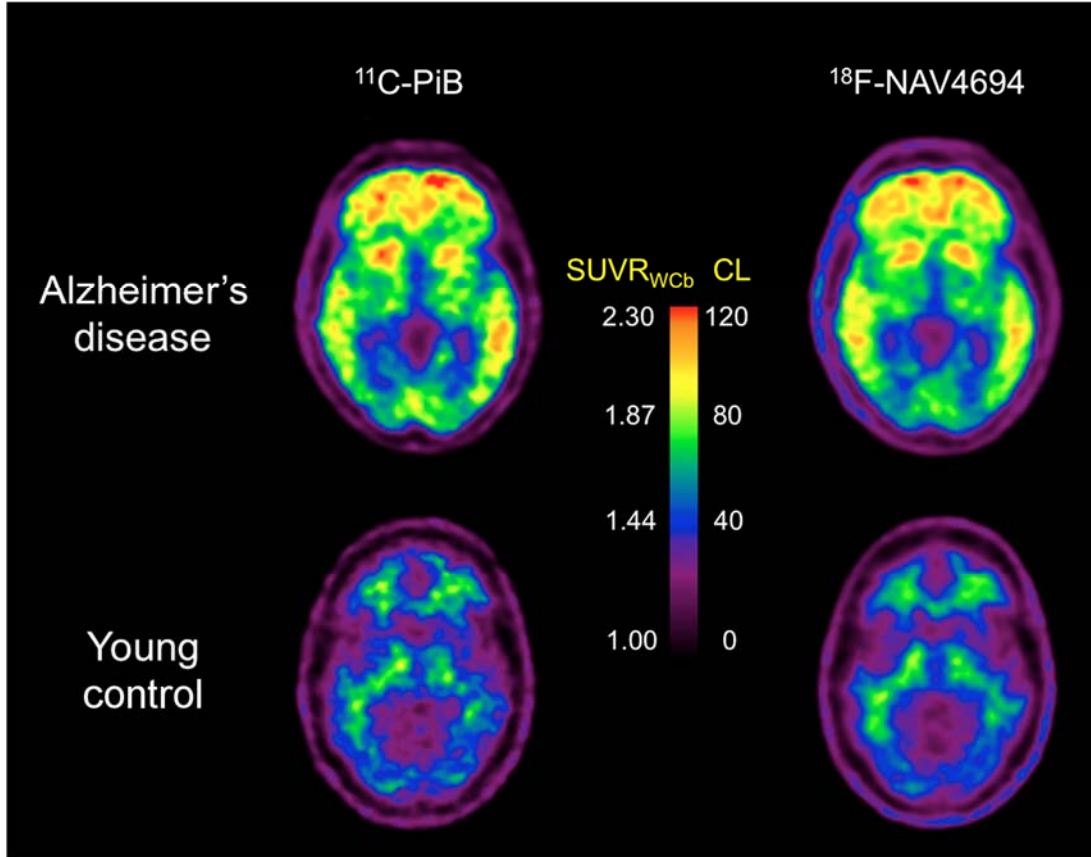


**Figure 3.** Same subject  $^{11}\text{C}$ -PiB and  $^{18}\text{F}$ -NAV4694 images in a patient with mild AD (top row) and a healthy young control (bottom row). The color scale is set to  $\text{SUVR}$  units using the Centiloid method with whole cerebellum reference region and to the matching Centiloid units.

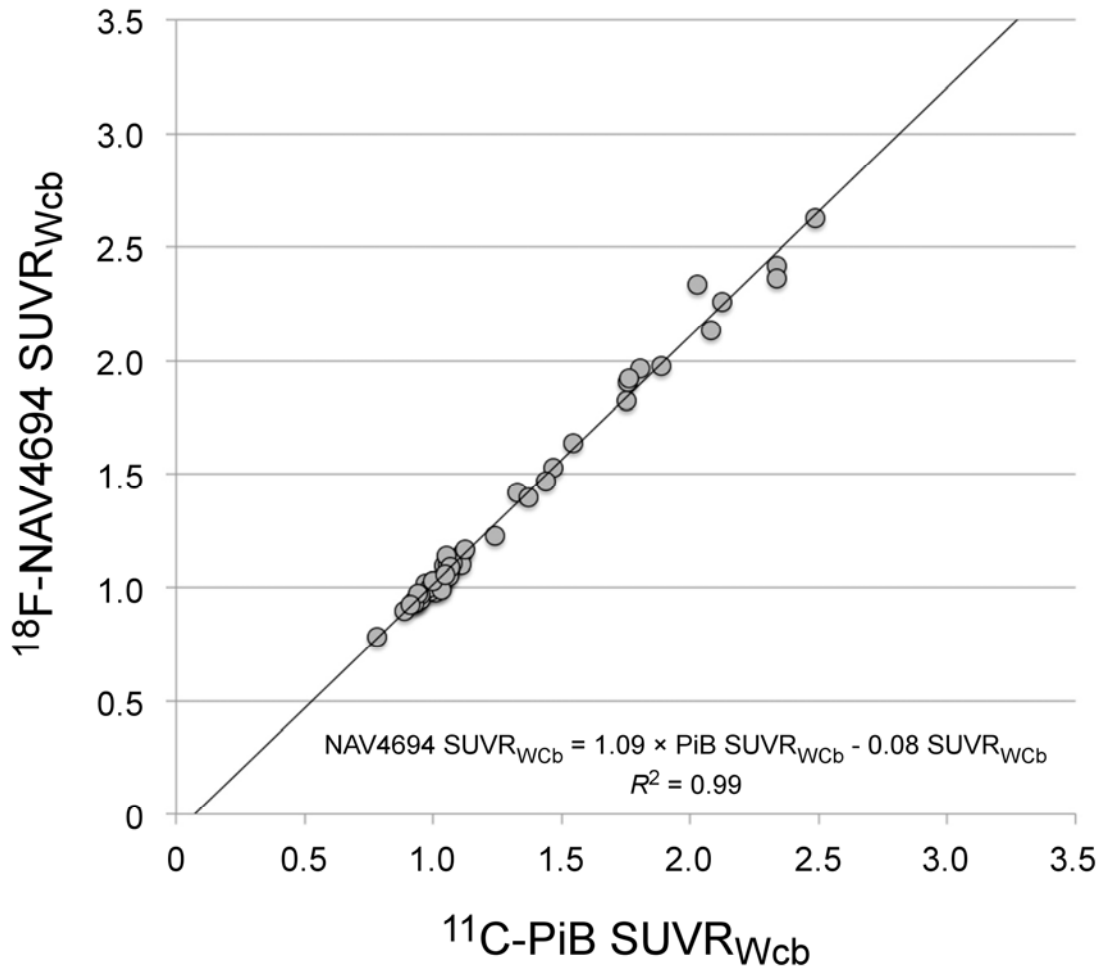


**Figure 4.** Plot of the paired  $^{11}\text{C-PiB SUVR}$  (X-axis) and  $^{18}\text{F-NAV4694 SUVR}$  for each subject. SUVR were calculated by the standard Centiloid method with the standard large single cortical region of interest and whole cerebellum reference region.

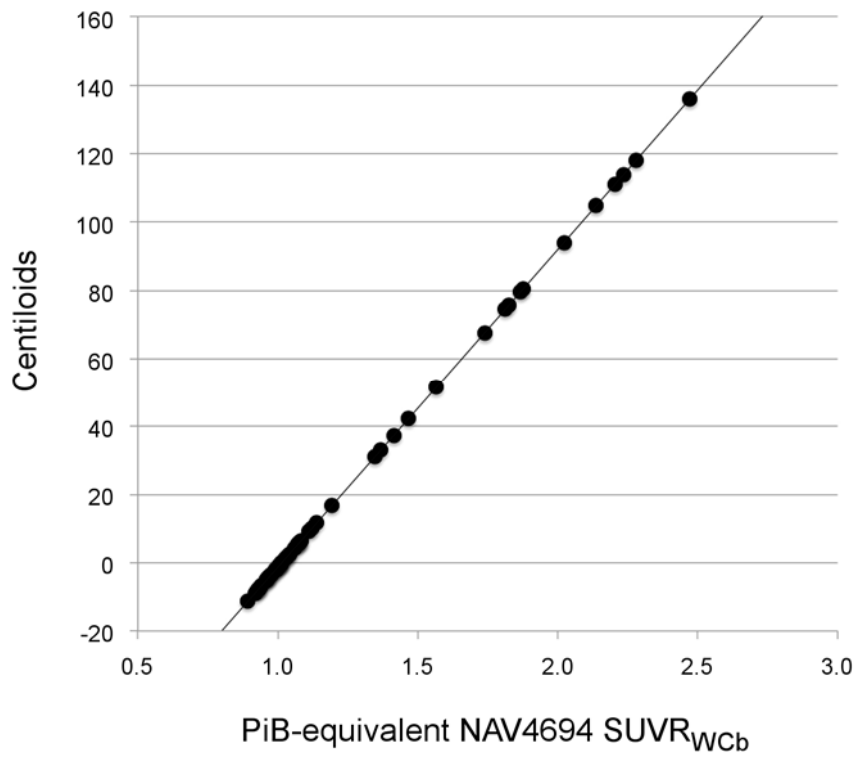


**Figure 5.** NAV4694 SUVR after conversion to the equivalent PiB SUVR X-axis) plotted against the Centiloid value for each PiB SUVR demonstrating good spread of the data points across the Centiloid range.